JOURNAL OF SOLID STATE CHEMISTRY 17, 353–361 (1976)

Proton Conduction in Triethylenediamine- and Hexamethylenetetramine-Sulfate

T. TAKAHASHI, S. TANASE, O. YAMAMOTO, AND S. YAMAUCHI

Department of Applied Chemistry, Faculty of Engineering, Nagoya University, Nagoya 464, Japan

Received December 31, 1974; in revised form, October 21, 1975

The electrical conductivities of the triethylenediamine- and hexamethylenetetramine-sulfuric acid systems have been measured and comparatively high electrical conductivities were found in the solid state. The protonic nature of charge carriers was confirmed by an electrolysis experiment and an EMF measurement. In the electrolysis experiment the evolution of hydrogen gas was found to be directly proportional to the electrical charge passed across the crystal and in the EMF measurement the cell potential followed the Nernst equation.

1. Introduction

The mechanism of proton migration in hydrogen-bonded materials and their dielectric properties have received considerable attention for a number of years. Knowledge of charge transfer properties in hydrogen-bonded materials is not only of major importance for understanding many biophysical processes in the biological systems (*1*) but also of great use for their practical applications. In particular, the solid electrolytes exhibiting high proton conductivity are of great interest as the electrolyte for fuel and electrolysis cells (*2*) and p(H_2) meters (*3*), and as hydrogen gas filters for refining hydrogen. In our laboratory, high-conductivity proton conductors in the solid state have been studied, and the triethylenediamine– and hexamethylenetetramine–sulfuric acid systems were found to have relatively high proton conductivity in the temperature range above several tens of degrees (centigrade). In particular, the electrical conductivity of the new compound in the triethylenediamine–sulfuric acid system, $C_6H_{12}N_2 \cdot \frac{3}{2}H_2SO_4$, was about $3 \times 10^{-5}\ \Omega^{-1}\ cm^{-1}$ at 100°C and about $1 \times 10^{-3}\ \Omega^{-1}\ cm^{-1}$ at 200°C. Though the conductivity of this compound is lower than that of H_3OClO_4 (*4*), which exhibits the highest proton conductivity at room temperature in the solid state ever reported, H_3OClO_4 decomposes to H_2O and $HClO_4$ at about 50°C while $C_6H_{12}N_2 \cdot \frac{3}{2}H_2SO_4$ can be stable up to 200°C.

2. Experimental

Triethylenediamine- and hexamethylenetetramine-sulfate were precipitated by adding concentrated sulfuric acid (>95%) to the alcoholic solution of triethylenediamine ($C_6H_{12}N_2$) and hexamethylenetetramine ($C_6H_{12}N_4$). After standing at room temperature for 1 day, the precipitate was filtered before being washed by pure solvent, and dried in a vacuum desiccator with phosphorus pentoxide for several hours. In these syntheses, the ratios of the amount of sulfuric acid to the amines were changed to obtain the sulfates containing various amounts of sulfate ion. The content of sulfate ion in the sample was determined by the usual gravimetric analysis. The specific gravity of the sulfate was measured using the pycnometer method. The dc and ac conductivities of solid triethylenediamine- and hexamethylenetetramine-sulfate were measured using pellet samples with silver

electrodes and a guard ring (*5*). The sample was pressed under a pressure of about 4 t/cm^2 to form a pellet about 3 mm in thickness and 13 mm in diameter. Both sides of the electrodes were kept in contact by a steel spring. The conductivity cell was placed in a large glass bottle which was evacuated for dehydration. The temperature was measured by an alumel–chromel thermocouple. The dc conductivity was measured using a regulated power supplier, a standard resistor, and an electrometer (Ohkura Denki Co.). When the resistance of the specimen is smaller than 100 kΩ, the ac conductivity was measured with 1 kHz-conductance bridge (Andoh Denki Co.). In the resistance range of 100 kΩ to 10 kΩ, the conductivities measured by dc and ac were almost identical within an experimental error. Powder X-ray diffraction patterns were obtained with Geiger flex D-2F (Rigaku Denki Co.).

Infrared absorption spectra were measured in dry air with JASCO DS-402G ir spectrometer by the KBr pellet method at room temperature in the wavenumber range of 200–4000 cm^{-1}. The proton transport number was determined by an electrolysis method with Schmidt's coulometer (*6*) and EMF method with a hydrogen concentration cell (*3*, *7*, *8*). In the former case, applying high dc voltage of 50 to 150 V, a dc current was passed through the crystal at 50°C with mercury electrodes to measure the volume of hydrogen gas evolved at the cathode. The coulombs passed through the cell were measured with the help of solid-state coulometer named MEMORIODE (Sanyo Electric Co.; *9*). The evolved gases were analyzed by gas chromatograph (Yanagimoto MFG Co. Model GCG-200) using argon as carrier gas. An EMF cell of the type,

$$Pt, H_2\,(P_1\,atm)|sample|Pt, H_2\,(P_2\,atm),$$

was used to measure the proton transport number. The cell assembly is shown in Fig. 1. The platinized platinum nets were used as electrodes. The gas tightness of two compartments was obtained by using a heat resistant silicone rubber O-ring. The used cell construction made it possible to maintain different atmospheres of flowing gas on both sides of the pellet. The different partial hydrogen

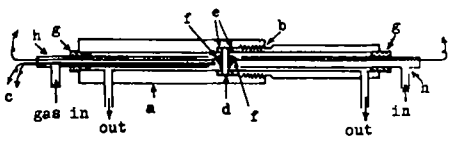

FIG. 1. EMF cell assembly. a, Teflon tube; b, close screw; c, alumel–chromel thermocouple; d, pellet; e, silicone rubber O-ring; f, platinum electrode contact; g, rubber plug; h, glass tube.

pressures on each side of the pellet were obtained by using a flow of about 60 cm^3/min of Ar–H_2 gas mixture with known compositions. Before use, the gas was dried by means of molecular sieves and phosphorus pentoxide. Small traces of oxygen were removed by copper nets heated at 600°C. The EMF of the gas concentration cell was measured by means of a digital voltmeter with an input impedance of 10^9 Ω (Takeda Riken Co.).

3. Results and Discussion

3.1. Formation of Triethylenediamine Sulfate and Hexamethylenetetramine sulfate

In general, the amine–H_2SO_4 system gives many types of sulfates having various contents of sulfuric acid. For example, four types of sulfates, $NH_3 \cdot \frac{1}{2}H_2SO_4$, $NH_3 \cdot H_2SO_4$, $NH_3 \cdot \frac{3}{2}H_2SO_4$, and $NH_3 \cdot 2H_2SO_4$, have been found in the NH_3–H_2SO_4 system. However, no work on the $C_6H_{12}N_2$–H_2SO_4 systems has been done previously. The ratio of H_2SO_4 to $C_6H_{12}N_2$, x, in triethylenediamine sulfate prepared in our laboratory was measured as a function of the amount of sulfuric acid added to a solution containing 3 g of $C_6H_{12}N_2$ in 100 ml of methanol and it is shown in Fig. 2. The value of x increases from 1 to 2 as the amount of H_2SO_4 increases to indicate that at least two types of sulfate, namely, $C_6H_{12}N_2 \cdot H_2SO_4$ and $C_6H_{12}N_2 \cdot 2H_2SO_4$, may exist. X-ray diffraction analysis carried out at room temperature showed a single-phase pattern for the sample containing H_2SO_4 with the ratio of about 1, 1.5, and 2 to $C_6H_{12}N_2$ as shown in Fig. 3. These results indicate that three compounds, $C_6H_{12}N_2 \cdot H_2SO_4$, $C_6H_{12}N_2 \cdot \frac{1}{2}H_2SO_4$, and $C_6H_{12}N_2 \cdot 2H_2SO_4$, exist at room temperature in the $C_6H_{12}N_2$–H_2SO_4 system.

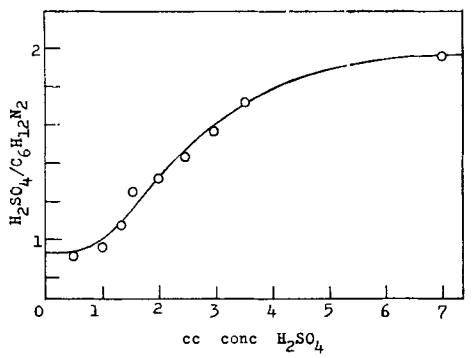

FIG. 2. Relation between the amount of concentrated sulfuric acid used and the content of H_2SO_4, x, in triethylenediamine sulfate, $C_6H_{12}N_2 \cdot xH_2SO_4$.

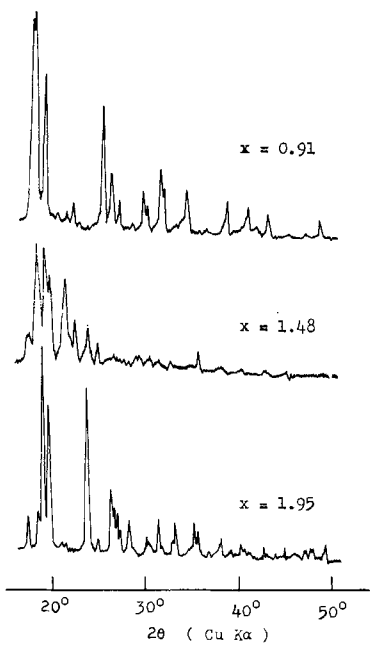

FIG. 3. X-ray diffraction patterns of triethylenediamine sulfates, $C_6H_{12}N_2 \cdot xH_2SO_4$, with various contents of sulfuric acid.

Differential thermal analysis (DTA) was carried out for these samples sealed in Vycor tube under vacuum. The melting points were found at 300°C for $C_6H_{12}N_2 \cdot 0.95H_2SO_4$, at 320°C for $C_6H_{12}N_2 \cdot 1.54H_2SO_4$, and at 250°C $C_6H_{12}N_2 \cdot 1.95H_2SO_4$ and the thermal peaks which appear to be the phase transition points were observed at 80°C for $C_6H_{12}N_2 \cdot 0.95H_2SO_4$ and at 140°C for $C_6H_{12}N_2 \cdot 1.95H_2SO_4$. However, these samples decomposed gradually above 220°C in air. X-ray diffraction patterns above 80°C for $C_6H_{12}N_2 \cdot 0.95H_2SO_4$ and above 140°C for $C_6H_{12}N_2 \cdot 1.95H_2SO_4$ were different from those obtained at room temperature, and their changes at the respective temperatures were reversible, which indicated that these temperatures are really the phase transition points. The infrared absorption spectra of triethylenediamine sulfates in the solid state are shown in Fig. 4a. Two absorption bands of SO_4^{2-} ion at 1110 and 610 cm^{-1} are observed in $C_6H_{12}N_2 \cdot 0.95H_2SO_4$ and the intensities of these bands decrease with increasing the content of H_2SO_4. Five absorption bands of HSO_4^- ion at 3000, 1190, 1070, 890, and 590 cm^{-1} are observed in $C_6H_{12}N_2 \cdot 1.54H_2SO_4$ and $C_6H_{12}N_2 \cdot 1.95H_2SO_4$. The broad absorption bands of ^+N–H···O stretching at 2500–2800 cm^{-1} and O–H···O stretching at about 3000 cm^{-1} are observed, and their intensities are nearly constant even when x is changed.

Previous works on the $C_6H_{12}N_4$–H_2SO_4 system have not been extensive, and two compounds, $C_6H_{12}N_4 \cdot \frac{1}{2}H_2SO_4$ and $C_6H_{12}N_4 \cdot H_2SO_4$, have been prepared (*10*). In Fig. 5, the content of H_2SO_4 in hexamethylenetetramine sulfate is shown as a function of the amount of sulfuric acid added to a solution containing 2 g of $C_6H_{12}N_4$ in 150 ml of ethanol. In this case, the largest ratio of H_2SO_4 to $C_6H_{12}N_4$ is 2.14. As shown in Fig. 6, X-ray diffraction investigations indicate that four compounds, $C_6H_{12}N_4 \cdot \frac{1}{2}H_2SO_4$, $C_6H_{12}N_4 \cdot H_2SO_4$, $C_6H_{12}N_4 \cdot \frac{3}{2}H_2SO_4$, and $C_6H_{12}N_4 \cdot 2H_2SO_4$, were found in the $C_6H_{12}N_4$–H_2SO_4 system. That is, two new compounds, $C_6H_{12}N_4 \cdot \frac{3}{2}H_2SO_4$ and $C_6H_{12}N_4 \cdot 2H_2SO_4$, were found in our laboratory. The melting points of these compounds measured in a sealed evacuated tube were 170°C for $C_6H_{12}N_4 \cdot 0.53H_2SO_4$, 146°C for $C_6H_{12}N_4 \cdot 1.02H_2SO_4$, 135°C for $C_6H_{12}N_4 \cdot 1.57H_2SO_4$, and 129°C for $C_6H_{12}N_4 \cdot 2.02H_2SO_4$. No phase transition was observed up to these melting points. In air, these compounds were decomposed above 160°C. The infrared absorption spectra of hexamethylenetetramine sulfate in the solid state are shown in Fig. 4b. Two absorption

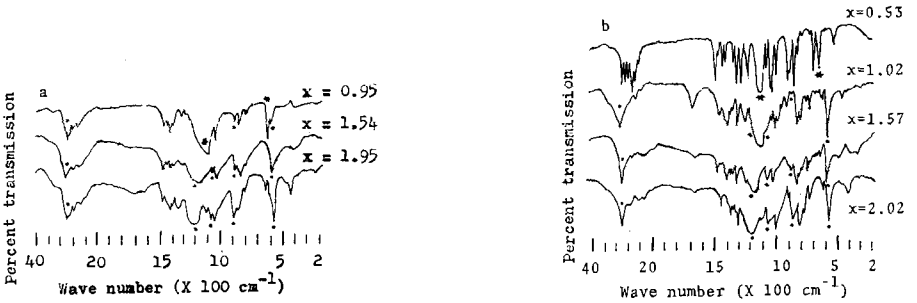

FIG. 4. Infrared absorption spectra of $C_6H_{12}N_2 \cdot xH_2SO_4$ and $C_6H_{12}N_4 \cdot xH_2SO_4$ in KBr pellet. (a) Triethylenediamine sulfate ($x = 0.95$, 1.54, and 1.95); (b) hexamethylenetetramine sulfate ($x = 0.53$, 1.02, 1.57, and 2.02). *, SO_4^{2-}; ·, HSO_4^-.

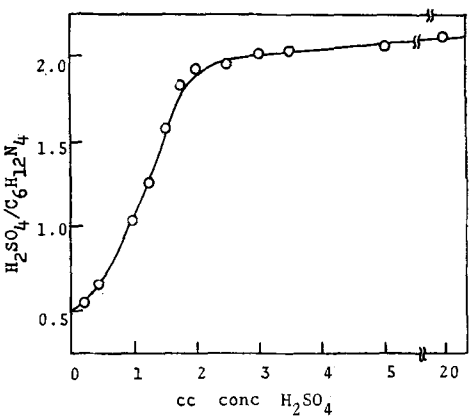

FIG. 5. Relation between the amount of concentrated sulfuric acid used and the content of H_2SO_4, x, in hexamethylenetetramine sulfate, $C_6H_{12}N_4 \cdot xH_2SO_4$.

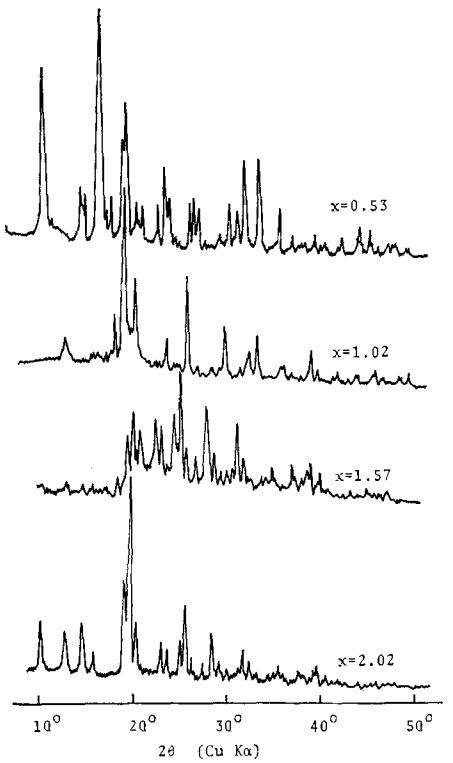

FIG. 6. X-ray diffraction patterns of hexamethylenetetramine sulfate, $C_6H_{12}N_4 \cdot xH_2SO_4$, with various contents of sulfuric acid.

bands of SO_4^{2-} ion at 1110 and 610 cm^{-1} are observed in $C_6H_{12}N_4 \cdot 0.53H_2SO_4$, and five absorption bands of HSO_4^- ion are observed at 3000, 1190, 1070, 890, and 590 cm^{-1} in $C_6H_{12}N_4 \cdot 1.02H_2SO_4$, $C_6H_{12}N_4 \cdot 1.57H_2SO_4$, and $C_6H_{12}N_4 \cdot 2.02H_2SO_4$. In the case of $C_6H_{12}N_4 \cdot 0.53H_2SO_4$, the absorption bands assigned to $^+$N–H stretching are observed in the region of 2450–2750 cm^{-1}, and in the case of $C_6H_{12}N_4 \cdot 1.02H_2SO_4$, $C_6H_{12}N_4 \cdot 1.57H_2SO_4$, and $C_6H_{12}N_4 \cdot 2.02H_2SO_4$, the broad absorption bands of $^+$N–H···O stretching at about 2400 cm^{-1} and O–H···O stretching at about 3000 cm^{-1} are found to increase gradually with increasing content of H_2SO_4. From these results, it is suggested that $C_6H_{12}N_4 \cdot H_2SO_4$, $C_6H_{12}N_4 \cdot \frac{3}{2}H_2SO_4$, and $C_6H_{12}N_4 \cdot 2H_2SO_4$ have two types of hydrogen bond of $\equiv{}^+$N–H···O– and –O–H···O–.

3.2. *Electrical Conductivity*

The polycrystallines of the sulfates were pressed in the shape of a pellet to measure the electrical conductivity because of the difficulty in obtaining single crystals of the sulfates. The porosities of the pellets calculated from the pycnometric density of the powder were less

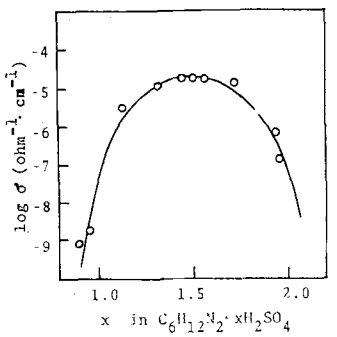

FIG. 7. Change of electrical conductivity of triethylenediamine sulfate, $C_6H_{12}N_2 \cdot xH_2SO_4$, with the content of H_2SO_4, x, at 100°C.

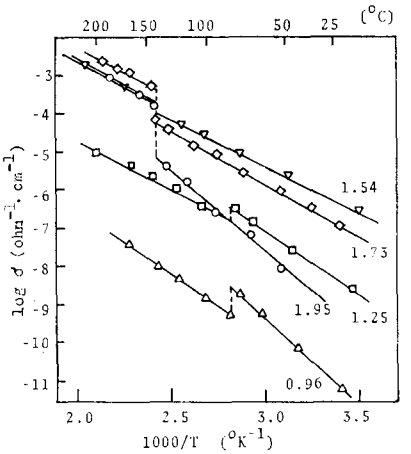

FIG. 8. Temperature dependence of electrical conductivity of triethylenediamine sulfate, $C_6H_{12}N_2 \cdot xH_2SO_4$ ($x = 0.96$, 1.25, 1.54, 1.73, and 1.95).

than 10%. For example, the density of the pellet of $C_6H_{12}N_2 \cdot 1.54H_2SO_4$ was found to be 1.54 g/cm³ which corresponded to 93% of the pycnometric density of the powder (1.659 g/cm³). The variation in conductivity with x value in $C_6H_{12}N_2 \cdot xH_2SO_4$ at 100°C is shown in Fig. 7. A maximum conductivity of $2.7 \times 10^{-5}\ \Omega^{-1}\ cm^{-1}$ is observed near the composition of $C_6H_{12}N_2 \cdot \frac{3}{2}H_2SO_4$. This result shows that the electrical conductivity of $C_6H_{12}N_2 \cdot \frac{3}{2}H_2SO_4$ at 100°C is higher than those of $C_6H_{12}N_2 \cdot H_2SO_4$ and of $C_6H_{12}N_2 \cdot 2H_2SO_4$. According to X-ray diffraction analysis, $C_6H_{12}N_2 \cdot xH_2SO_4$ ($1 < x < 1.5$) is a mixture of $C_6H_{12}N_2 \cdot H_2SO_4$ and $C_6H_{12}N_2 \cdot \frac{3}{2}H_2SO_4$, and $C_6H_{12}N_2 \cdot xH_2SO_4$ ($1.5 < x < 2$) is a mixture of $C_6H_{12}N_2 \cdot \frac{3}{2}H_2SO_4$ and $C_6H_{12}N_2 \cdot 2H_2SO_4$. Therefore, the conductivities of $C_6H_{12}N_2 \cdot xH_2SO_4$ increase with increasing x from 1 to 1.5 because the content of high-conductivity phase, $C_6H_{12}N_2 \cdot \frac{3}{2}H_2SO_4$, increases while they decrease with increasing x from 1.5 to 2 because the content of $C_6H_{12}N_2 \cdot \frac{3}{2}H_2SO_4$ decreases. The temperature dependence of conductivity of $C_6H_{12}N_2 \cdot xH_2SO_4$ with various ratios of H_2SO_4 to $C_6H_{12}N_2$ is shown in Fig. 8. For $C_6H_{12}N_2 \cdot 0.96H_2SO_4$ and $C_6H_{12}N_2 \cdot 1.25H_2SO_4$, an abrupt decrease of conductivity is observed near 80°C and for $C_6H_{12}N_2 \cdot 1.73H_2SO_4$ and $C_6H_{12}N_2 \cdot 1.95H_2SO_4$, an abrupt increase near 140°C, which coincide with the phase transition temperature observed by DTA. The activation energies for conduction of the triethylenediamine sulfates calculated from Arrhenius plot are shown in Table I. The activation energy for $C_6H_{12}N_2 \cdot 0.96H_2SO_4$ is comparable to those of $(NH_2CH_2COOH)_3 \cdot H_2SO_4$, NH_4ClO_4, $NH_2CONH_2 \cdot HNO_3$, and $(NH_4)_2SO_4$, as shown in Table I. These compounds have a ^+N–H···O hydrogen bond, and the proton can move through the hydrogen bond. Thus, the proton

TABLE I

OBSERVED ACTIVATION ENERGIES OF CONDUCTION IN TRIETHYLENEDIAMINE SULFATES, HEXAMETHYLENETETRAMINE SULFATES, AND SOME PROTON CONDUCTORS

Material	Activation energy (eV)		
$C_6H_{12}N_2 \cdot 0.96H_2SO_4$	0.90[a]		0.74[b]
$C_6H_{12}N_2 \cdot 1.54H_2SO_4$	0.53[a]		0.45[b]
$C_6H_{12}N_2 \cdot 1.95H_2SO_4$	0.95[a]		0.45[b]
$C_6H_{12}N_4 \cdot 0.53H_2SO_4$		1.76	
$C_6H_{12}N_4 \cdot 1.02H_2SO_4$		0.98	
$C_6H_{12}N_4 \cdot 1.57H_2SO_4$		1.23	
$C_6H_{12}N_4 \cdot 2.02H_2SO_4$		0.93	
KH_2PO_4 (*11*)	0.55		
Ice (*12*)	0.53		
$(NH_2CH_2COOH)_3 \cdot H_2SO_4$ (*13*)			1.26
NH_4ClO_4 (*14*)			0.85
$(NH_2)_2CO \cdot HNO_3$ (*15*)			1.08
$(NH_4)_2SO_4$ (*16*)			0.76

[a] From room temperature to phase transition points.
[b] Above phase transition points.

migration mechanism in $C_6H_{12}N_2 \cdot H_2SO_4$ will be similar to that of NH_4ClO_4. The existence of ^+N–H···O hydrogen bond in $C_6H_{12}N_2 \cdot H_2SO_4$ was suggested by ir measurements. The activation energy for $C_6H_{12}N_2 \cdot 1.54H_2SO_4$ is comparable to those of KDP and ice as shown in Table I. This result suggests that the proton migration mechanism in $C_6H_{12}N_2 \cdot \frac{3}{2}H_2SO_4$ will be similar to that of ice, that is, $C_6H_{12}N_2 \cdot \frac{3}{2}H_2SO_4$ has a three-dimensional hydrogen bond, O–H···O, and a proton can move through the hydrogen bond which is shown by ir measurements. In this case, a small change of the activation energy is observed above 140°C, which coincides with the phase transition temperature, and this change will be due to the fact that $C_6H_{12}N_2 \cdot 1.54H_2SO_4$ is a mixture consisting of a large amount of $C_6H_{12}N_2 \cdot \frac{3}{2}H_2SO_4$ and a small quantity of $C_6H_{12}N_2 \cdot 2H_2SO_4$. In the case of $C_6H_{12}N_2 \cdot 1.95H_2SO_4$, the activation energies of 0.45 and 0.95 eV were observed in the temperature range of 140 to 190 and 50 to 140°C, respectively. The former is comparable to that of $C_6H_{12}N_2 \cdot 1.54H_2SO_4$ and the latter to that of $C_6H_{12}N_2 \cdot 0.95H_2SO_4$. From these results, the proton migration mechanism in the high-temperature modification will be suggested to be similar to that of $C_6H_{12}N_2 \cdot \frac{3}{2}H_2SO_4$. According to the ir experiment of $C_6H_{12}N_2 \cdot 1.95H_2SO_4$ at room temperature, two types of hydrogen bond, O–H···O and ^+N–H···O, were recognized. Therefore, the protons in the low-temperature modification cannot move along the O–H···O hydrogen bond, but can move along the ^+N–H···O hydrogen bond. Infrared measurements of the high-temperature modification of $C_6H_{12}N_2 \cdot 2H_2SO_4$ have not been carried out; thus, it is not clear what type of hydrogen bond exists in this modification. However, from the activation energy for conduction the proton can be considered to move along O–H···O hydrogen bond.

The conductivities of $C_6H_{12}N_4 \cdot xH_2SO_4$ at 25°C are represented in Fig. 9 as a function of x. This result shows that the conductivity maximum is presented near $x = 2$, i.e., $C_6H_{12}N_4 \cdot 2H_2SO_4$ exhibits the highest conductivity among four compounds, $C_6H_{12}N_4 \cdot xH_2SO_4$ ($x = \frac{1}{2}$, 1, $\frac{3}{2}$, and 2). X-ray diffraction patterns

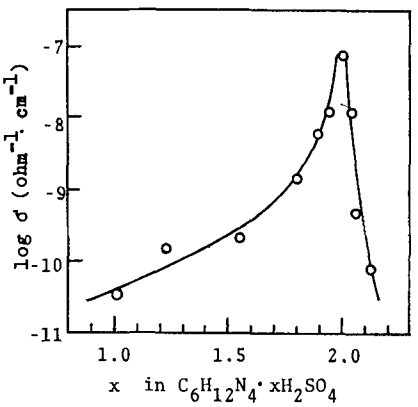

FIG. 9. Dependence of electrical conductivity of hexamethylenetetramine sulfate on the content of H_2SO_4, x, at 25°C.

and ir spectra of $C_6H_{12}N_4 \cdot (2+\delta)H_2SO_4$ ($\delta > 0$) were almost the same as those of $C_6H_{12}N_4 \cdot 2H_2SO_4$. From these results, it can be assumed that the excess of H_2SO_4 dissolves in the stoichiometric compound, $C_6H_{12}N_4 \cdot 2H_2SO_4$, and the conductivities of the solid solution, $C_6H_{12}N_4 \cdot (2+\delta)H_2SO_4$, decrease with increasing value of δ, that is, the excess of H_2SO_4 dissolved in $C_6H_{12}N_4 \cdot 2H_2SO_4$ retards the proton conduction in the crystal. The formation of the solid solution was suggested from the fact that the melting points became higher with increasing δ. The temperature dependence of conductivities of $C_6H_{12}N_4 \cdot 0.53H_2SO_4$, $C_6H_{12}N_4 \cdot 1.02H_2SO_4$, $C_6H_{12}N_4 \cdot 1.57H_2SO_4$, and $C_6H_{12}N_4 \cdot 2.02H_2SO_4$ is shown in Fig. 10. The activation energy of hexamethylenetetramine sulfates calculated from the temperature dependence of conductivity is shown in Table I. The activation energies of $C_6H_{12}N_4 \cdot 1.02H_2SO_4$, $C_6H_{12}N_4 \cdot 1.57H_2SO_4$, and $C_6H_{12}N_4 \cdot 2.02H_2SO_4$ have almost the same magnitude as those of $(NH_2CH_2COOH)_3 \cdot H_2SO_4$ and NH_4ClO_4 in which the migrating proton is considered to be generated from $[NH_3CH_2COOH]^+$ or $[NH_4]^+$. Therefore, it is suggested that in $C_6H_{12}N_4 H_2SO_4$, $C_6H_{12}N_4 \cdot \frac{3}{2}H_2SO_4$, and $C_6H_{12}N_4 \cdot 2H_2SO_4$, the proton generated from the $[C_6H_{12}N_4 \cdot H]^+$ group is able to migrate easily along the ^+N–H···O hydrogen bond. However, the activation energy of $C_6H_{12}N_4 \cdot 0.53H_2SO_4$ is larger than those of $C_6H_{12}N_4 \cdot xH_2SO_4$ with

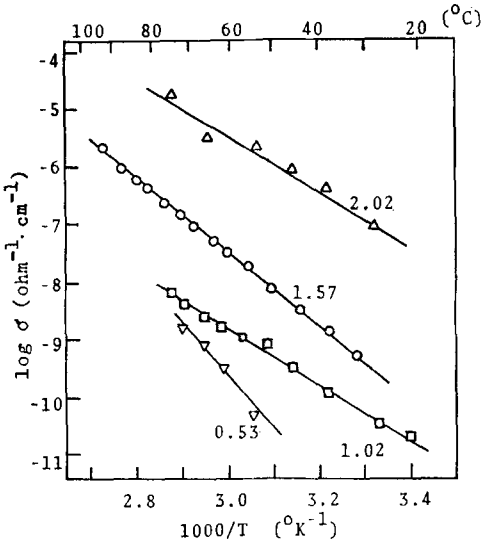

FIG. 10. Temperature dependence of electrical conductivity of hexamethylenetetramine sulfate, $C_6H_{12}N_4 \cdot xH_2SO_4$ ($x = 0.53$, 1.02, 1.57, and 2.02).

$x = 1.02$, 1.57, and 2.02. The low electrical conductivity and high activation energy for $C_6H_{12}N_4 \cdot \frac{1}{2}H_2SO_4$ will be due to the fact that this compound has no remarkable hydrogen bond which is suggested by ir measurements.

In the above discussion, the proton conduction mechanism in triethylenediamine- and hexamethylenetetramine-sulfate are considered by merely the results of ir measurements and the activation energies for conduction. To discuss the information of their crystal structures further, the NMR measurements and the dielectric dispersions may be necessary. These studies are now under investigation in our laboratory.

3.3 Transport Number

The determination of charge carriers in the triethylenediamine- and hexamethylenetetramine-sulfate systems was performed by the electrolysis and EMF methods. The electrolysis experiment was carried out for $C_6H_{12}N_2 \cdot 1.54H_2SO_4$ and $C_6H_{12}N_4 \cdot 2.02H_2SO_4$, which have the highest conductivities in the triethylenediamine- and hexamethylenetetramine-sulfate systems, respectively. Before measurement, in order to remove the adsorbed water in the sample and to make mercury and kerosene saturate with hydrogen gas, preelectrolysis was carried out for 1 day. The electrical conductivity of the sample was calculated from the potential drop and the current passed through the electrolysis cell gradually decreased with electrolysis time and became constant after 1 day. The conductivity was comparable to that measured under a vacuum. After these treatments, the volume of hydrogen gas evolved was measured by Schmidt's equipment and was plotted against the charge transported across the crystal. As shown in Figs. 11a and b, the hydrogen evolution rate is 0.116 ml H_2 STP/C, which agreed within experimental error with the calculated value considering that the sample was pure protonic conductor. The gas chromatograph spectra of the evolved gas are compared with the spectra obtained with pure hydrogen and air in Fig. 12 to show that the

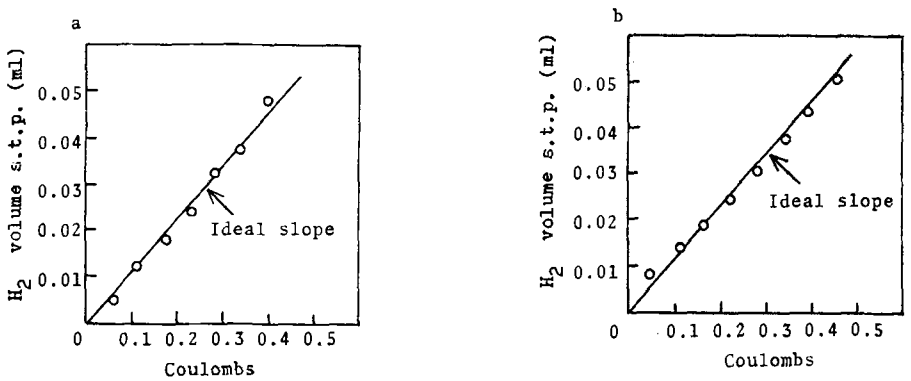

FIG. 11. Volume of evolved H_2 plotted against the charge passed through the pellet at 50°C. (a) $C_6H_{12}N_2 \cdot 1.54H_2SO_4$; (b) $C_6H_{12}N_4 \cdot 2.02H_2SO_4$.

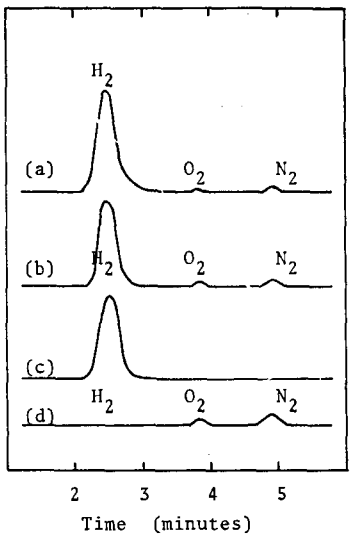

FIG. 12. Gas chromatograph spectra of (a) gas collected at the cathode of the electrolysis cell with the pellet of hexamethylenetetramine sulfate, (b) gas with the pellet of triethylenediamine sulfate, (c) pure hydrogen, and (d) air.

evolved gas was hydrogen, though it contained a small amount of air which was introduced at the time of withdrawal of the evolved gas from the coulometer. Some gaseous products were also released at the anode during electrolysis; analysis showed them to be oxygen and nitrogen.

The EMF of cells of types (I) and (II),

$$\mathrm{Pt, H_2|C_6H_{12}N_2\cdot 1.54H_2SO_4|Pt, H_2, Ar} \quad \text{(I)}$$

$$\mathrm{Pt, H_2|C_6H_{12}N_4\cdot 2.03H_2SO_4|Pt, H_2, Ar} \quad \text{(II)}$$

are represented in Fig. 13. The absence of thermal EMF was verified by filling both electrode compartments with pure hydrogen gas. In cell (I) at 201°C, the response of the EMF to change of gas composition was fast. Furthermore, this EMF was found to be stable for a long time. Assuming that the electrodes are completely reversible, the ionic transport number can be determined from $t_i = E/E_{\text{theor}}$, where E is the experimental EMF and E_{theor} is the thermodynamically predicted Nernst expression:

$$E_{\text{theor}} = \frac{RT}{2F} \ln \frac{P_{\mathrm{H_2\,(anode)}}}{P_{\mathrm{H_2\,(cathode)}}}.$$

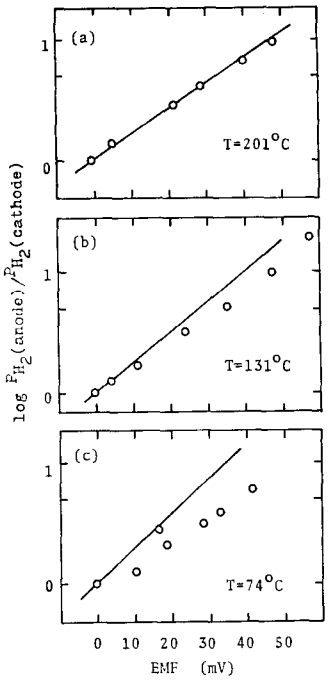

FIG. 13. EMF of cells with platinized platinum net electrodes. (a), (b) For triethylenediamine sulfate at 201 and 131°C, respectively; (c) for hexamethylenetetramine sulfate at 74°C. Solid line, theoretical values.

From the data given in Fig. 13, it can be calculated that the Nernst expression is obeyed for triethylenediamine sulfate, so that the ionic transport number, i.e., the protonic transport number, is unity within an experimental error. In cell (I) at 131°C and in cell (II) at 70°C, the EMF responses to the change of gas composition were slow and the EMF was changed with time, which will be attributed to the high resistivity of samples and the poor reversibility of the electrodes at lower temperatures.

4. Conclusions

Three compounds, $\mathrm{C_6H_{12}N_2\cdot xH_2SO_4}$ ($x = 1, \frac{3}{2}$, and 2), have been found in the triethylenediamine–sulfuric acid system and four compounds, $\mathrm{C_6H_{12}N_4\cdot xH_2SO_4}$ ($x = \frac{1}{2}$, 1, $\frac{3}{2}$, and 2), in the hexamethylenetetramine–sulfuric acid system. Among these compounds, $\mathrm{C_6H_{12}N_2\cdot \frac{3}{2}H_2SO_4}$ and $\mathrm{C_6H_{12}N_4\cdot 2H_2SO_4}$ exhibited relatively high proton conductivity. Their

proton transport numbers were nearly unity and the conduction mechanism could be explained on the basis of hydrogen bonds in the crystal.

References

1. N. RIEHL, *Naturwissenschaften* **43**, 145 (1956).
2. R. L. COSTA AND P. G. GRIMES, *Chem. Eng. Progr.* **63**, 56 (1967).
3. J. BRUININK AND B. KOSMEIJER, *J. Phys. Chem. Solids* **34**, 897 (1973).
4. A. POTIER AND D. ROUSSELET, *J. Chim. Phys.* **70**, 873 (1973).
5. L. B. HARRIS, *J. Appl. Phys.* **41**, 1883 (1970).
6. V. H. SCHMIDT, *J. Sci. Instrum.* **42**, 889 (1965).
7. F. A. KRÖGER, *J. Chem. Phys.* **51**, 4025 (1969).
8. P. N. KRISHNAN, I. YOUNG, AND R. E. SALOMON, *J. Phys. Chem.* **70**, 1595 (1966).
9. T. TAKAHASHI AND O. YAMAMOTO, *J. Appl. Electrochem.* **3**, 129 (1973).
10. H. I. BEILSTEIN, S. 586.
11. M. O'KEEFFE AND C. T. PERRINO, *J. Phys. Chem. Solids* **28**, 211 (1967).
12. M. EIGEN, L. DE MAEYER, AND H. CH. SPATZ, *Ber. Bunsenges. Phys. Chem.* **68**, 19 (1964).
13. G. ROYAL, B. MORLON, AND G. GODEFROY, *C.R. Acad. Sci. Ser. B.* **275**, 353 (1972).
14. P. W. M. JACOBS AND WEE LAM NG, *J. Phys. Chem. Solids* **33**, 2021 (1972).
15. T. R. NARAYANAN KUTTY AND A. R. VASUDEVA MURTHY, *Indian J. Chem.* **11**, 253 (1973).
16. V. H. SCHMIDT, *J. Chem. Phys.* **38**, 2783 (1963).